The orientation distribution of single joint sets

TERRY ENGELDER[1] & JEAN DELTEIL[2]

[1] *Department of Geosciences, Pennsylvania State University, University Park, PA 16802, USA (e-mail: engelder@goesc.psu.edu)*

[2] *Geosciences Azur, UMR 6526, Université de Nice – Sophia Antipolisu, 250 Rue Albert Einstein, Sophia Antipolis, F-06560 Valbonne, France*

Abstract: Poles from line samples of systematic joint sets scatter about a mean pole because joints are neither perfectly planar nor parallel, and because measurement instruments are imprecise. Definition of a single joint set can be based solely on its orientation distribution and this distribution is assessed using two statistical parameters: square root of the circular variance (approximately equal to the standard deviation σ for two-dimensional (2D) data) and cone of confidence (α_{95} for 3D data). The distribution for joints generated in the absence of tectonic deformation is well clustered with $\sigma = 1.7°$ and $\alpha_{95} = 0.48°$ based on a bootstrap sample of 50. Jointing associated with various fold styles show less clustering: the kink of a fault-bend fold ($\sigma = 6.1°$ and $\alpha_{95} = 1.7°$), basement-cored anticline ($\sigma = 3.5°$ and $\alpha_{95} = 1.5°$), regional joint set transected by a basement-cored anticline ($\sigma = 5.2°$ and $\alpha_{95} = 1.8°$) and a buttress anticline ($\sigma = 4.3°$ and $\alpha_{95} = 1.7°$). Jointing associated with local faulting tends to show even less clustering: a Cretaceous marl ($\sigma = 8.3°$ and $\alpha_{95} = 2.4°$) and a glauconitic sandstone ($\sigma = 8.6°$ and $\alpha_{95} = 2.2°$). The latter sample was drawn from two overlapping joint sets, indicating that distribution data greater than $\alpha_{95} = 2.2°$ may signal overlapping joint sets.

How can geologists identify joint sets from line samples such as tunnels, drill cores, borehole logs and outcrop faces along road and stream cuts? In line samples (especially in the case of borehole logs), orientation and position of joints may be the only data available. On outcrop faces and along drill core, joint-surface morphology may be of further help in distinguishing joint sets (e.g. Savalli, 2003). Even if orientation and position are the only data, identification of different joint sets can be important for detailed modelling of fractures for fluid-flow and stability analyses.

To answer the question posed above, geologists require knowledge of the orientation distribution of joints populating a single set. If joints propagate within an isotropic, homogeneous rock under the influence of an homogeneous remote driving stress (an homogeneous stress field has straight stress trajectories at the scale of the sample; Means 1976), the joint set is a collection of systematic joints, planar and parallel, with poles projecting to one point on a stereonet (Hodgson 1961). In the Earth, however, stress fields are commonly spatially and temporally inhomogeneous (i.e. their stress trajectories curve as demonstrated by elastic analyses, such as those of Ode 1957, and at the microscopic and smaller mesoscopic scales rock is quite inhomogeneous, e.g. Kranz 1979). The presence of joints and joint tips further complicates the local stress field (e.g. Olson & Pollard 1989). Although many joints have fairly smooth surfaces, possibly a direct consequence of subcritical crack growth, others are irregular because they formed by dynamic crack growth.

Joints of a set are neither completely planar nor perfectly parallel (e.g. Dyer 1988; Rawnsley *et al.* 1992). For this reason, the definition of a collection of joints populating a single joint set must be based on some statistical inferences. In geological media, there will never be absolute agreement on how to identify members of a single joint set nor will there be absolute certainty that all members of a collection of joints belong to the same set. In these instances, statistical inferences are helpful if it is necessary to define joint sets based on orientation data alone. Even then, a line sample crossing curving joints will yield orientation data that cannot be easily grouped into one single set.

The objective of this chapter is to present some statistical criteria that characterize the orientation distribution of joints in a set. This exercise then allows us to examine the degree of clustering of the poles to joints propagating in different tectonic settings, particularly from line samples in which the orientation and position of joints are the only available data. First, we consider the precision of the measurement instrument, usually a geological compass of some sort if samples are collected from scanlines along outcrop faces. Next, we make use of two statistics, kurtosis and the cone of confidence, to compare the degree of joint clustering from various tectonic settings. For a control sample we use data from relatively isotropic, homogeneous rock where joints are driven under the influence of a reasonably homogeneous stress field. Then, we calculate these two statistics for joint sets from tectonically complex settings where the driving stress might have been inhomogeneous in space or

From: COSGROVE, J. W. & ENGELDER, T. (eds) 2004. *The Initiation, Propagation, and Arrest of Joints and Other Fractures*. Geological Society, London, Special Publications, **231**, 285–297. 0305-8719/04/$15

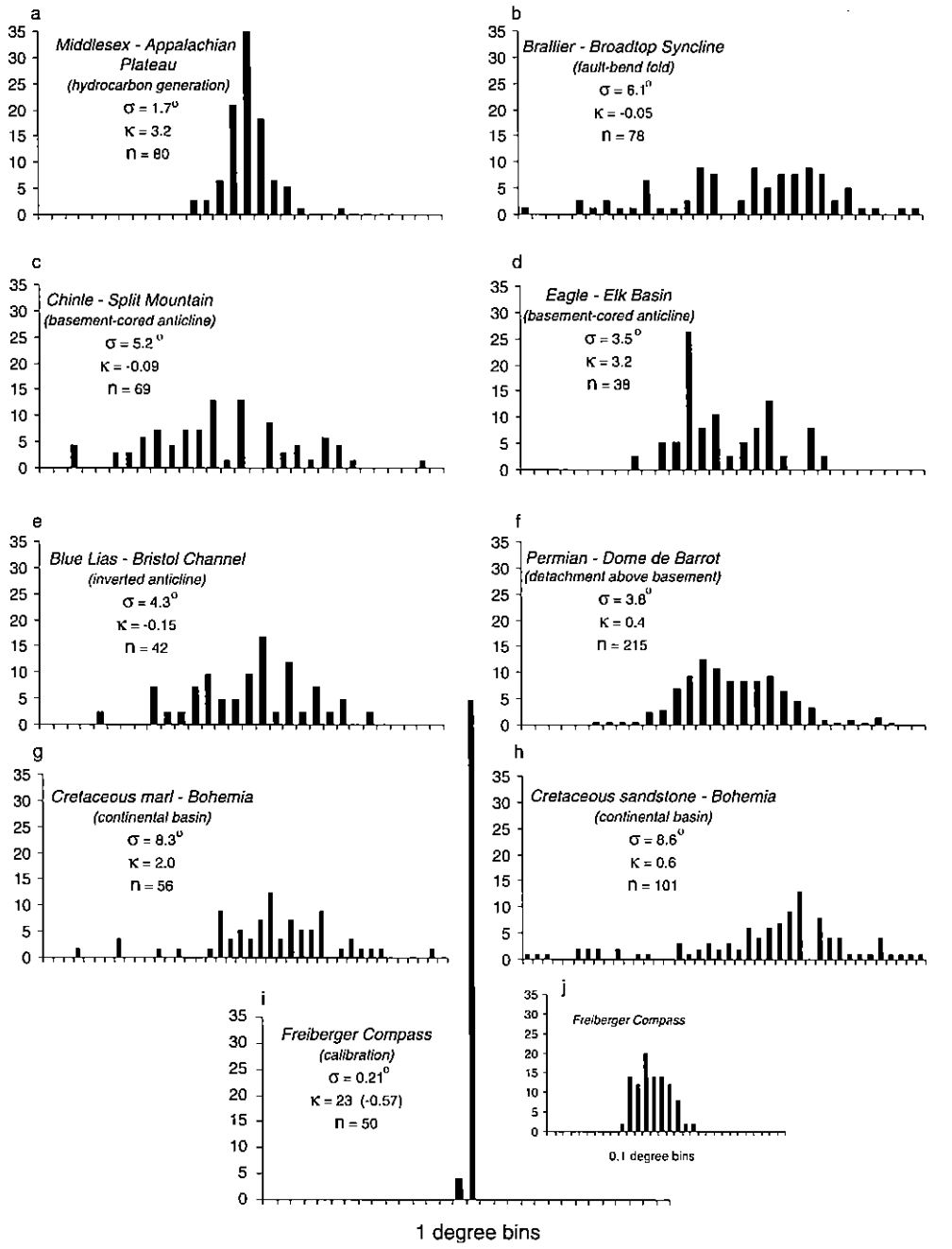

Fig. 1. Histograms of the strike of joints from one bed in eight exposures representing different tectonic environments throughout the world. The data are normalized to 100% so that the vertical scale on each histogram is divided into 5% intervals. Each bin is 1° except for the insert for data from the Freiberger compass which is divided into 0.1° bins. σ, standard deviation; κ, kurtosis; *n*, number of data. Source of the data: (**a**) Devonian Middlesex Formation, New York (Hagan 1997); (**b**) Devonian Brailler Formation, Pennsylvania (Ruf *et al.* 1998); (**c**) Triassic Chinle Formation, Utah (Silliphant *et al.* 2002); (**d**) Cretaceous Eagle Formation, Wyoming (Engelder *et al.* 1997); (**e**) Jurassic Blue Lias, UK (Engelder & Peacock 2001); (**f**) Permian of the Dome de Barrot (this paper); (**g**) and (**h**) Cretaceous Jizera Formation of Bohemia (this paper). (**i**) and (**j**) The Freiberger compass (used for all data sampling except that of Hagan 1997, who used a Silva).

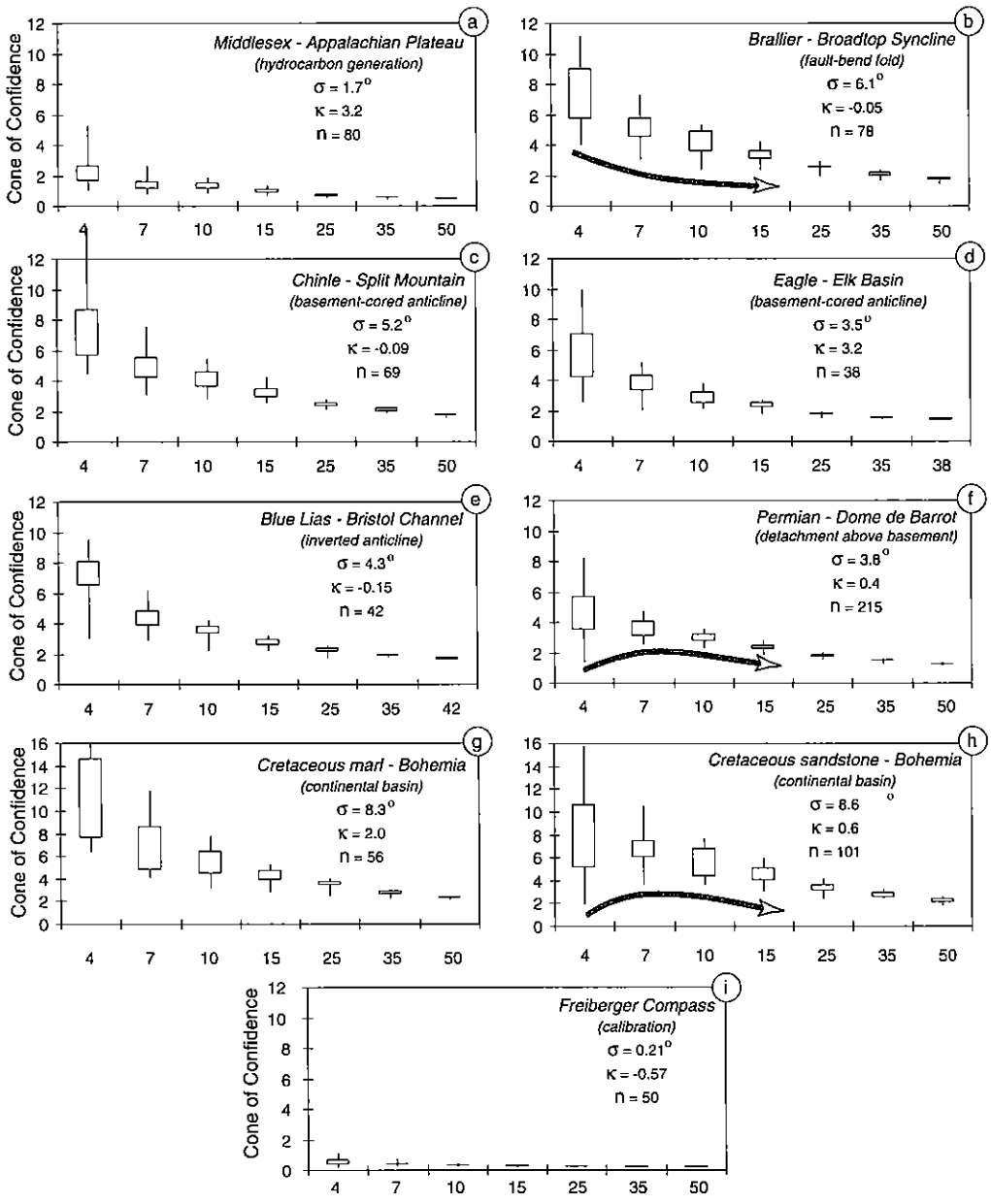

Fig. 2. Box and whisker diagram for the distribution of the α_{95} cone of confidences for 21 draws of random samples ($4 \leq n \leq 50$). Each box defines the α_{95} for the 25th and 75th percentile. The tips of the whiskers define the maximum and minimum α_{95}. For the sources of the data see caption to Figure 1.

shale prior to Alleghenian deformation (Lash *et al.* 2004). Other than a bedding fissility and concretions (e.g. McConaughy & Engelder 1999), this black shale was devoid of internal structures at the time of joint propagation. We examine orientation data collected by Hagen (1997) from this ENE joint set within the Finger Lakes District of New York State.

A scanline, placed on the pavement surface of a streambed, crossed 80 joints of the ENE set in a distance of 33 m (outcrop STE-01–AY). The 2D statistics

develops incrementally through time (Fischer & Wilkerson 2000). Here the stress field may be thought of as varying temporally rather than spatially, as is the case of a fixed hinge fold. We examine two cases for Laramide folds. In one example a pre-existing joint set is transected by later folding and in the other example jointing is coaxial with folding.

Split Mountain anticline. The Split Mountain anticline is a W-plunging forced fold that formed during the Eocene uplift of the eastern Uinta Mountains (Hansen 1986). Transected joints (i.e. systematic joints that strike at an angle to the present fold axis trend) occur on the flanks of Split Mountain (Silliphant *et al.* 2002). The common orientation on both flanks for these WNW-striking joints is inconsistent with joints driven by a synfolding stretch normal to the direction of highest curvature. Silliphant *et al.* (2002) concluded that these joints propagated as a systematic set prior to Laramide folding because a smaller dispersion of the poles to these transected joints occurs when they are rotated with bedding to their 'prefold' orientation. Post-folding joints are wing cracks growing from the tips of prefolding joints (Wilkins *et al.* 2001).

Prefolding joints are particularly well developed in the Triassic Chinle Formation, a fluvial clastic rock with interbedded overbank mud deposits and channel sandstones of irregular thickness. Relative to both the black shale of the Middlesex Formation and the regular bedding of the distal turbidites in the Brallier Formation, the sandstone beds in Chinle Formation are discontinuous and quite inhomogeneous. Even if regional jointing in the Chinle were driven by a homogeneous stress field, a relatively larger σ is expected for these joints because of the irregular bedding. Indeed, the transected joints in the Chinle Formation at Split Mountains display $\sigma =$ 5.2° and $\kappa = -0.09$ (Fig. 1c). Again, this bed was selected because more than 50 joints were sampled in a single scanline.

Twenty-one draws of four orientation data collected at random from the Chinle data set give an α_{95} of between 4.4° and 14.1°, with a median of 6.8°. As with the Middlesex and Brallier, when 10 samples were collected at random in the Chinle, $\alpha_{95} < \sigma$ for a collection of strike data (Fig. 2c).

Elk Basin anticline. Elk Basin is a breached anticline, typical of Laramide (i.e. Late Cretaceous–Eocene) basement-involved folds in the northern portion of the Big Horn Basin, Montana–Wyoming (McCabe 1948). Structural relief on the Elk Basin anticline is about 1500 m. Deep seismic sections show a basement thrust to the ENE, causing an asymmetric drape of cover rocks with a forelimb dip in excess of 30° to the ENE, and the backlimb dipping 23° to the WSW (Bally 1983; Stone 1993). The structural evolution of the Elk Basin anticline extends from late Cretaceous sedimentation through Palaeocene to Eocene basement thrusting. Of 72 outcrops sampled within sandstone beds, 67 are cut by one or more systematic joint sets, with systematic strike joints being far more common than dip joints (Engelder *et al.* 1997). In some outcrops two joint sets develop with dihedral angles of 10°–25° and abutting relationships that indicate a clockwise reorientation of the bedding-parallel stress axes during fold development. Joints coaxial to the strike of the fold at Elk Basin are considered to have a synfolding origin as a consequence of fold-induced stretching over the crest of the fold.

The strike joints in one bed of the Eagle Formation of Elk Basin display $\sigma = 3.5°$ and $\kappa = 3.2$ (Fig. 1d). When comparing these statistics to those found in the Brallier Formation or the Appalachian Valley and Ridge and the Chinle Formation of Split Mountain, we might conclude that sample population of joints within the Eagle are drawn from one joint set and that this set propagated more or less at one time during axis-normal stretching accompanying fold growth.

Twenty-one draws of four orientation data collected at random from the Eagle data set give an α_{95} between 2.6° and 9.9°, with a median of 5.4° (Fig. 2d). The axis of the Elk Basin is curved, reflecting the spoon-shaped basement fault over which the Cretaceous clastic rocks are draped. Because of the curved axis, it is not appropriate to use the α_{95} statistic to test whether or not the joint set is coaxial to the fold.

Comparing our two Laramide folds, the range of α_{95} for draws of four data from the Chinle at Split Mountain is the larger. This was not expected because prefolding joints sets like those found in the Middlesex have a relatively small α_{95} (Fig. 2a) One source for the large α_{95} at Split Mountain is infilling by joint growth during folding, as documented by Wilkins *et al.* (2001). Renewed growth of prefolding joints as wing cracks adds to the dispersion of the orientation data. If so, then it might be argued that our sample of Chinle is an example of an incipient second joint set (i.e. wing cracks) overprinting a single, early set. This would also be the reason for the slightly negative κ at Split Mountain.

Limb of a buttress anticline

Inversion in the Bristol Channel Basin during Pyrenean tectonics includes reverse-reactivated normal faults with hanging-wall buttress anticlines (Nemčok *et al.* 1995). At Lilstock Beach, one of several joint sets (i.e. the J_3 set of Engelder & Peacock 2001) in Lower Jurassic Blue Lias limestone beds clusters about the trend of the hinge of the

looking at a natural spectrum of orientations from one set of veins or whether there are two vein sets that signal a small change in the orientation of the driving stress. If the latter is true then at least one of the vein sets is not coaxial with the total finite strain in this tectonite, an issue that we deal with later in this chapter.

The veins in the Permian section of the Dome de Barrot display $\sigma = 3.8°$ and $\kappa = 0.4$ (Fig. 1f). When $\kappa \leq 1$, there is the possibility that more than one joint set contributed to the sample. In the case of Dome de Barrot, two closely oriented vein sets appear to have formed based on the histogram for vein strike that shows two peaks separated by 5° (Fig. 1f). If, in fact, this exposure contains two vein sets, then the σ is not large relative to that for a single vein set.

The α_{95} for a random draw of four orientation data from the Permian marl is between 1.4° and 8.3°, with a median of 4.7° (Fig. 2f). Other than the clustering of joints within the Middlesex black shale, no suite of α_{95} data has smaller minimum (i.e. a tighter cluster) for four random samples. However, the unusual characteristic to the α_{95} sampling for the Dome de Barrot is that the range of α_{95} for seven random samples has a minimum value (i.e. 2.5°) that is nearly double in size from the smallest α_{95} in the four-sample draw (i.e. arrow in Fig. 2f). The minimum value for α_{95} in all other samples discussed so far has decreased when seven-sample draws are taken (i.e. arrow in Fig. 2b). When going from four-sample draws to seven-sample draws at Dome de Barrot, this increase in α_{95} is a consequence of sampling two vein sets. When taking some small samples, all data may, by random chance, come from one of the two sets and are, therefore, tightly clustered. This results in a small α_{95}. Other small samples take data from both joint sets and have a concomitant larger α_{95}. A tight cluster also reflects the fact that both of the vein sets in the Dome de Barrot are relatively homogeneous in orientation, a characteristic found only in the Middlesex black shale. Seven-sample draws all included data from both vein sets in this example.

Cretaceous basin, Bohemian Massif

The high stand of the Cretaceous seas flooded a large basin on the NE side of the Bohemian Massif in the Czech Republic. This Cretaceous basin is elliptical with its long axis trending NW–SE. On the Bohemian Massif the Turonian Jizera Formation is characterized by marls, interlayered marly siltstones and glauconitic sandstone. Steeply dipping faults are common within the Cretaceous basin. Post-Cretaceous jointing pervades the Turonian section to the extent that most exposures along the Orlice River are well jointed with more than one joint set. The most prominent joint set strikes NE–SW, which is across the axis of the Cretaceous basin but the joints are in the strike orientation relative to NW-verging thrusts of the western Carpathians, which are located to the SE.

The character of jointing within marls appears quite different from the jointing within the glauconitic sandstone beds. The vertical growth of joints in the more homogeneous marls is extensive, much like the vertical joints in the Middlesex Formation of the Appalachian Plateau. A closer inspection, however, reveals that the individual joints are not as systematic as those of the Middlesex. In contrast, the joints of the glauconitic sandstone beds include a well-developed set that is contained within individual beds between 20 and 40 cm thick. More widely spaced joints may be traced vertically through several beds. Like their counterparts in the thick marls, joints within the glauconitic sandstone beds appear systematic on first glance but are also found to be less systematic upon closer inspection.

Jointing in the thicker marls was sampled near the railway station at Usti nad Orlici and about 100 m west of a high-angle normal fault. Jointing in the glauconitic sandstone beds was sampled along the River Orlice at Chocen, about 500 m from the nearest prominent normal fault. Both exposures are cliff faces so we were unable to observe joints in plan view. Both samples proved to have a larger σ than any of the previously described data sets (Fig. 1g, h). A positive κ (=2.0) in the thicker marl supports the premise that we did measure just one joint set but this set is characterized by a large dispersion. The joints with the glauconitic sandstone beds show a prominent peak but have a smaller κ. The smaller κ is largely a consequence of several joints that were about 20° anticlockwise from the peak.

The α_{95} for a random sample of four orientation data from the marl is between 6.3° and 19.2°, with a median of 10.8°. This large range reflects the relatively non-systematic nature of joint development within the marls, presumably because of the exposure's proximity to the nearby steeply dipping fault. The α_{95} for a random sample of four orientation data from the glauconitic sandstone beds is between 1.9° and 16.7°, with a median of 8.5°. This reflects the more systematic organization of jointing in the bedded sandstones. Like our sample from the Dome de Barrot, random samples of seven data within the glauconitic sandstone have a larger α_{95} (= 3.7°) than the minimum for four random samples. In fact, 50 random samples are required before the α_{95} is reduced below the minimum for four random samples. By applying the same rational developed for orientation data from Dome de Barrot, we conclude that the glauconitic sandstone contains more than one joint set. The second set is not as common but can be seen in the histogram for the glauconitic sandstone (Fig. 1h).

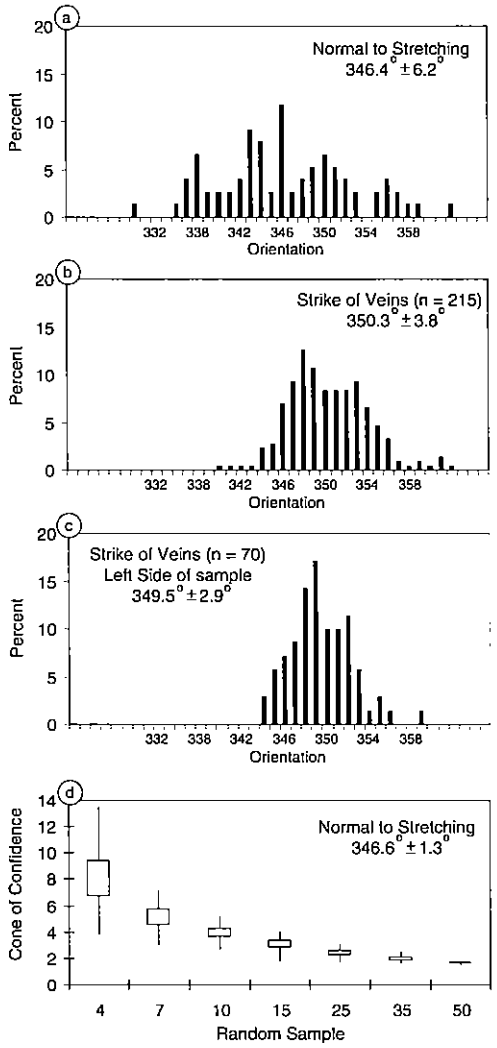

Fig. 4. Histograms of the direction of (**a**) layer-parallel shortening identified as the normal line to the long direction of each hexagonal block defined by mudcracks, (**b**) and (**c**) the strike of veins, and (**d**) box and whisker diagram for the distribution of the α_{95} cone of confidence for 21 draws of random samples ($4 \leq \leq 50$) of the layer-parallel shortening from the Dome de Barrot. Each box defines the α_{95} for the 25th and 75th percentile.

and the mudcracks are not coaxial. This is a conclusion that is not evident with a visual inspection (Fig. 3). However, a plot of the orientation of the veins in the plane of bedding relative to the orientation of the axes of shortening in bedding show a misalignment (Fig. 4). Even if the maximum bin (i.e. 348°) were taken as the orientation of one vein set, we see that this orientation is outside the cone of confidence for the layer-parallel shortening.

In brief, most parts of the Dome de Barrot have just one vein set. Even when there are two events of vein development, neither strictly corresponds to the direction of layer-parallel shortening as indicated by the mudcracks. Therefore, we accept the hypothesis that veins and layer-parallel shortening are not coaxial. However, we are struck by the extent to which the stress state remained in approximately the same orientation (i.e. ±2°) over time.

Conclusions

Joint sets can be distinguished using line sampling of joints for which only orientation and position data are available. Systematic joint sets propagating in a non-tectonic regime show a relatively small cone of confidence (i.e. $\alpha_{95} = 0.48°$) and a peaked, postive kurtosis. Syntectonic joints or early joints that have been tilted with the growth of a fold have a larger cone of confidence (i.e. $\alpha_{95} = 1.5°–1.8°$) and less peaked but still postive kurtosis. When two closely oriented joint sets appear in the same sample set the α_{95} can increase as the selection of random samples from the entire population of joints in an exposure increases from, say, four to seven.

This work was supported by Pennsylvania's State's Seal Evaluation Consortium (SEC) and a fellowship from the French–American Foundation, Paris. P. Gilliespie, A. Whitaker, and J. Cosgrove are thanked for constructive reviews.

References

BALLY, A. W. 1983. *Seismic Expression of Structural Styles*. American Association of Petroleum Geologists: Studies in Geology Series, **15**.

DAVIS, J. C. 1986. *Statistics and Data Analysis in Geology*. John Wiley, New York.

DYER, R. 1988. Using joint interactions to estimate paleostress ratios. *Journal of Structural Geology*, **10**, 685–699.

EFRON, B. & GONG, G. 1983. A leisurely look at the bootstrap, the jackknife and cross-validation. *American Statistician*, **37**, 36–48.

ENGELDER, T. & PEACOCK, D. 2001. Joint development normal to regional compression during flexural-slow folding: The Lilstock buttress anticline, Somerset, England. *Journal of Structural Geology*, **23**, 259–277.

ENGELDER, T., GROSS, M. R. & PINKERTON, P. 1997. Joint development in clastic rocks of the Elk Basin anticline, Montana–Wyoming. *In*: HOAK, T., KLAWITTER, A. & BLOMQUIST, P. (eds) *An Analysis of Fracture Spacing Versus Bed Thickness in a Basement-involved Laramide Structure*. Rocky Mountain Association of Geologists 1997 Guidebook. Rocky Mountain Association of Geologists, Denver, CO, 1–18.

cline, Utah: constraints placed by transected joints. *Journal of Structural Geology*, **24**, 155–172.

STONE, D. S. 1993. Basement-involved thrust-generated folds as seismically imaged in the subsurface of the central Rocky Mountain foreland. *In*: SCHMIDT, C.J., CHASE, R.B. & ERSLEV, E.A. (eds) *Laramide Basement Deformation in the Rocky Mountain Foreland of the Western United States*. Geological Society of America, Special Papers, **280**, 271–318.

SUPPE, J. 1983. Geometry and kinematics of fault-bend folding. *American Journal of Science*, **283**, 684–721.

WALPOLE, R. & MYERS, R. 1993. *Probability and Statistics for Engineers and Scientists*. Prentice-Hall, Englewood Cliffs, NJ.

WILKINS, S. J., GROSS, M. R., WACKER, M., EYAL, Y. & ENGELDER, T. 2001. Faulted joints: kinematics, displacement–length scaling relationships and criteria for their interpretation. *Journal of Structural Geology*, **23**, 315–327.

WISE, D. U. & MCCRORY, T. A. 1982. A new method of fracture analysis; azimuth versus traverse distance plots. *Geological Society of America Bulletin*, **93**, 889–897.

ENGELDER, T., HAITH, B. F. & YOUNES, A. 2001. Horizontal slip along Alleghanian joints of the Appalachian plateau: evidence showing that mild penetrative strain does little to change the pristine appearance of early joints. *Tectonophysics*, **336**, 31–41.

ERSLEV, E. A. 1991. Trishear fault-propagation folding. *Geology*, **19**, 617–620.

FAILL, R. T. 1973. Kink band folding, Valley and Ridge Province, Pennsylvania. *Geological Society of American Bulletin*, **84**, 1289–1314.

FAURE-MURET, A. 1955. *Etudes géologiques sure le massif de l'Argentera–Mercantour et ses envelopes sédimentaires*. Service de la Carte Géologique de France, Mémoires.

FISCHER, M.P. & WILKERSON, S. 2000. Predicting the orientation of joints from fold shape: results of pseudo-three-dimensional modeling and curvature analysis. *Geology*, **28**, 15–18.

FISCHER, M., GROSS, M. R., ENGELDER, T. & GREENFIELD, R. J. 1995. Finite element analysis of the stress distribution around a pressurized crack in a layered elastic medium: Implications for the spacing of fluid-driven joints in bedded sedimentary rock. *Tectonophysics*, **247**, 49–64.

FISHER, N. I., LEWIS, T. L. & EMBLETON, B. J. J. 1987. *Statistical Analysis of Spherical Data*. Cambridge University Press, Cambridge.

FISHER, R. W. 1953. Dispersion on a sphere. *Proceedings of the Royal Society of London*, **A217**, 295–305.

FRY, N. 1979. Random point distributions and strain measurements in rocks. *Tectonophysics*, **60**, 89–105.

GRAHAM, R. H. 1978. Quantitative deformation studies in the Permian rocks of Alpes-Maritimes. *Mémoires du Bureau de Recherches Géologiques et Minières*, **91**, 219–238.

GOGUEL, J. 1936. *Description tectonique de la bordure des Alpes de la Boéone au Var*. Service de la Carte Géologique de France, Mémoires.

HAGIN, P. N. 1997. *Joints spacing statistics in thick, homogeneous shales of the Catskill Delta complex on the Appalachian plateau: Finger lakes Region, New York*. B.S. thesis, Pennsylvania State University.

HANSEN, W. R. 1986. History of faulting in the eastern Uinta Mountains, Colorado and Utah. *In*: STONE, D. S. (ed.) *New Interpretations of Northwest Colorado Geology*. Rocky Mountain Association of Geologists, Denver, CO, 229–246.

HENRY, B. 1973. Studies of microstructures, anisotropy of magnetic susceptibility and paleomagnetism of the Permian Dome de Barrot (France): paleotectonic and paleosedimentological implications. *Tectonophysics*, **17**, 61–72.

HODGSON, R. A. 1961. Regional study of jointing in Comb Ridge–Navajo mountain area, Arizona and Utah. *AAPG Bulletin*, **45**, 1–38.

KRANZ, R. L. 1979. Crack–crack and crack–pore interactions in stressed granite. *International Journal of Rock Mechanics and Mining Science*, **16**, 37–47.

LASH, G. LOEWY, S. & ENGELDER, T. 2004. Preferential jointing of Upper Devonian black shale, Appalachian Plateau, USA: evidence supporting hydrocarbon generation as a joint-driving mechanism. *In*: COSGROVE, J. W. & ENGELDER, T. (eds) *The Initiation, Propagation, and Arrest of Joints and Other Fractures*. Geological Society, London, Special Publications, **231**, 129–151.

MARDIA, L. 1972. *The Statistics of Orientation Data*. Academic Press, London.

MCCABE, W. S. 1948. Elk Basin Anticline, Park County, Wyoming, and Carbon County, Montana. *AAPG Bulletin*, **32**, 52–67.

MCCONAUGHY, D. T. & ENGELDER, T. 1999. Joint interaction with embedded concretions: Joint loading configurations inferred from propagation paths. *Journal of Structural Geology*, **21**, 1049–1055.

MCELHINNY, M. W. 1964. Statistical significance of the fold test in paleomagnetism. *Geophysical Journal of Astronomical Society*, **8**, 338–340.

MEANS, W. D. 1976. *Stress and Strain – Basic Concepts of Continuum Mechanics for Geologists*. Springer, New York.

NARR, W. 1991. Fracture density in the deep subsurface: Techniques with application to Point Arguello Oil Field. *AAPG Bulletin*, **75**, 1300–1323.

NEMČOK, M. BAYER, R. & MILIORIZOS, M. 1995. Structural analysis of the inverted Bristol Channel Basin: implications for the geometry and timing of fracture porosity. *In*: BUCHANAN, J. G. & BUCHANAN, P. G. (eds) *Basin Inversion*. Geological Society, London, Special Publications, **88**, 355–392.

ODE, H. 1957, Mechanical analysis of the dyke pattern of the Spanish Peaks area, Colorado. *Geological Society of America Bulletin*, **68**, 567–576.

OLSON, J. E. & POLLARD, D. D. 1989. Inferring paleostress from natural fracture patterns: A new method. *Geology*, **17**, 345–348.

POLLARD, D. D. & SEGALL, P. 1987. Theoretical displacements and stresses near fractures in rock: with applications to faults, joints, veins, dikes, and solution surfaces. *In*: ATKINSON, B. (ed.) *Fracture Mechanics of Rock*. Academic Press, Orlando, FL, 227–350.

RAMSAY, J. G. & HUBER, M. I. 1983. *The Techniques of Modern Structural Geology: Volume 1: Strain Analysis*. Academic Press, Orlando, FL.

RAWNSLEY, K. D., RIVES, T., PETIT, J.-P. HENCHER, S. R. & LUMSDEN, A. C. 1992. Joint development in perturbed stress fields near faults. *Journal of Structural Geology*, **14**, 939–951.

RUF, J. C. RUST, K. A. & ENGELDER, T. 1998. Investigating the effect of mechanical discontinuities on joint spacing. *Tectonophysics*, **295**, 245–257.

SAVALLI, L. 2003. *Mechanisms controlling rupture front geometries during joint propagation in layered clastic sediments*. MS thesis, Pennsylvania State University.

SHELDON, P. 1912. Some observations and experiments on joint planes. *Journal of Geology*, **20**, 53–70.

SIDDANS, A. W. B. 1980. Compaction, metamorphisme et structurologie des argilites permiennes dans les Alpes-Maritimes (France). *Revue de Geologie Dynamique et de Geographie Physique*, **22**, 279–292.

SIDDANS, A. W. B., HENRY, B., KLIGFIELD, R., LOWRIE, A., HIRT, A. & PERCEVAULT, M. N. 1984. Finite strain patterns and their significance in Permian rocks of the Alpes Maritimes (France). *Journal of Structural Geology*, **6**, 339–368.

SILLIPHANT, L. J., ENGELDER, T. & GROSS, M. R. 2002. The state of stress in the limb of the Split Mountain anti-

An application of α_{95}: a bootstrap test for coaxial deformation

Standard techniques for strain analysis, such as the Fry (1979) centre-to-centre technique, are effective tools for measuring the orientation of the strain ellipse. However, in its original form, it offers no mechanism for assessing confidence in the orientation. We can develop a sense of confidence through a calculation of the cone of confidence for orientation data. We will apply this technique to measure the relationship between the orientation of veins in the Permian rocks of the Dome de Barrot and the strain ellipse as recorded in mudcracks (i.e. Siddans *et al.* 1984). We focus on this hypothesis because the veins of the Dome de Barrot appear to be coaxial with the flattening direction of the mudcracks and, yet the veins show no tendency to be buckled or otherwise deformed. Hence, the veins may post-date the syn-flattening strain of the mudcracks.

Coaxial deformation

Increments of strain are coaxial only if there is no component of rotational strain at any stage during the deformation (Ramsay & Huber 1983). Theoretically, coaxial strain takes place only if the driving stress field remains stationary and its principal axes correlate with the principal axes of strain throughout the deformation. In this case the finite strain is characterized by pure shear with principal axes of strain remaining in the same orientation during each increment of strain. In geological time, the tectonic stress field can change a great deal relative to a local coordinate system and consequently there has usually been some element of rotational (i.e. non-coaxial) strain when large finite strain is found in rock. Yet, tectonic stress within the Dome de Barrot appears to have remained stable from the time of the flattening of mudcracks until the time of propagation of the veins that cut the mudcracks.

There is a distinction between the strain recorded by joints and strain recorded by other structures. A joint is coaxial with one increment of strain small enough to be considered infinitesimal, whereas other strain markers record the orientation of the total-strain ellipsoid if they were present at the start of strain. A crack–seal vein may show many increments of growth and it is thus a finite-strain marker. Fibres normal to a vein wall indicate that the crack–seal vein remained coaxial with the tectonic stress field. Oblique fibres in a crack–seal vein are an indication that recracking is, in fact, guided within the vein and that the crack driving stress is no longer coaxial with the vein. A vein with oblique fibres is commonly associated with a spectrum of other veins that are misaligned, thus indicating a change in the orientation of the driving stress relative to the coordinate system of early veins.

Deformation within the Dome de Barrot: coaxial or non-coaxial?

Within the Permian section of Dome de Barrot strain indicators include mudcracks (Graham 1978), reduction spots (Siddans 1980), veins (Siddans *et al.* 1984), remanent magnetization (Henry 1973) and anisotropy of magnetic susceptibility (Siddans *et al.* 1984). In the Dome de Barrot region, in particular, veins overprint deformed mudcracks in an orientation that gives the appearance of two coaxial mesoscopic structures (Fig. 3). The problem is that with the unaided eye, we cannot tell whether these two structures are really coaxial. This is one of the reasons why we are particularly interested in understanding how a single fracture set might look from a statistical point of view. If we have a rigorous definition of a single fracture set from a simple statistical test, then we can determine the extent to which we are confident that the two mesoscopic structures are coaxial.

Using the veins and mudcracks in the Permian rocks of the Dome de Barrot, we can test for the stability of the finite-strain ellipsoid by correlating vein orientation with the finite-strain ellipse from the mudcracks. Rather than using the conventional centre-to-centre techniques for determining the orientation of the finite-strain ellipse for mudcracks (i.e. Fry 1979), we use a technique that gives some estimate of the confidence that we have in the orientation of the finite ellipse. To develop a sense of statistical confidence in the orientation of strain on the plane of bedding, we use the long axes of the blocks between the mudcracks. Each has a long dimension defined as the distance between sharp corners of the irregular hexagon that constitutes individual blocks defined by mudcracks. Because the initial shape of the hexagonal blocks is irregular, very few of the longest dimensions actually sit in the orientation of the finite-strain ellipse. However, with a large sample of the orientation of long dimensions of the many blocks, a confidence can be assigned to the calculated axis of maximum shortening (i.e. the direction perpendicular to the long axes of the hexagonal blocks). We can test for the reliability of our estimate of the stretching direction using the same α_{95} calculation that we applied to the poles to joints (Fig. 4).

In the sample coordinate system, the statistically averaged mean vector for the long axis of one section of the strain ellipsoid of the mudcracks is $346.4° \pm 1.3°$ ($n = 77$). The veins as a whole sample have a statistically averaged vector mean pole of $348.8° \pm 0.6°$ ($n = 215$). The α_{95} for the mudcracks does not encompass the vector mean pole for the veins nor do the two α_{95} cones overlap. The veins

Lilstock buttress anticline. In horizontal and gently N-dipping beds, J_3 joints (*c.* 295°–285° strike) are rare, while other joint sets indicate an anticlockwise sequence of development (Engelder & Peacock 2001). In the steeper S-dipping beds, J_3 joints are the most frequent in the vicinity of the reverse-reactivated normal fault responsible for the buttress anticline. The J_3 joints strike parallel to the fold hinge, and their poles tilt to the south when bedding is restored to horizontal. This southward tilt aims at the trajectory of regional σ_1 during Pyrenean tectonics.

Joint clustering in the Blue Lias at Lilstock is interesting for two reasons. First, these rocks record dramatic swings in orientation of joint sets in the vicinity of normal faults, much like those reported by Rawnsley *et al.* (1992) for other places along the English coastline. However, J_3 joints were not observed near the normal faults. Second, this is also an example, like the Brallier, where there is a non-orthogonality between joints and bedding. Here the mechanism for tilting joints relative to bedding is believed to be a shear traction set up by regional stresses rather than local bending stresses, as was the case for the Brallier (Engelder & Peacock 2001). Nevertheless, these joints, like those in the Brallier and Eagle formations of Elk Basin, are in the strike orientation.

The strike joints of the J_3 set in the Blue Lias of the Lilstock buttress anticline display $\sigma = 4.3°$ and $\kappa = -0.15$ (Fig. 1e). The negative κ is indicative of a range of orientation data that witness the relative inhomogeneity of the stress field at the time of joint propagation during the development of the buttress anticline at Lilstock. Small samples of joints within the Blue Lias compare with those from the Brallier, Chinle and Eagle formations. Twenty-one draws of four orientation data collected at random produces a range for α_{95} between 2.9° and 9.5°, with a median of 7.4°. Here, again, is such a large α_{95} that one cannot be sure with four measurements whether J_3 is coaxial with the buttress anticline at Lilstock Beach. Larger samples demonstrate that this is true.

An application of α_{95}: a bootstrap test for two overlapping fracture sets

In many instances, the assessment of joints and other fracture sets is based on their appearance in cliff faces and other places where good exposures in plan view (i.e. pavements) are not available. With just vertical faces available, visual inspection is rarely sufficient to recognize the presence of more than one joint set when two sets have formed at a small dihedral angle. Here statistical inferences are necessary. We first develop a bootstrap test for discriminating multiple joint sets in an outcrop where pavement view confirms the presence of two closely oriented joint sets. Then, we apply this bootstrap test to exposures where pavement surfaces are unavailable.

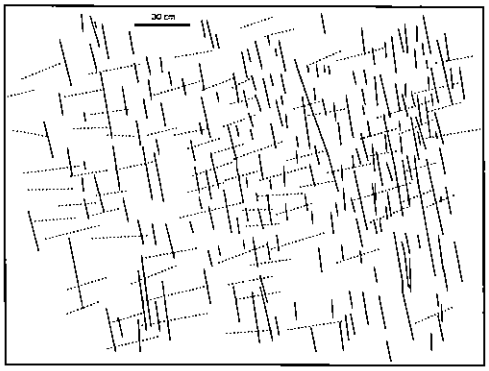

Fig. 3. Tracing of veins (solid lines) and the longest dimension of the hexagonal blocks defined by mudcracks (dashed lines) from the Dome de Barrot. This sample comes from a large block that is not in place, hence the absolute orientation of the veins and finite strain are know only from adjacent outcrops (see Siddans *et al.* 1984).

Dome de Barrot, Alpes Maritimes

We start with an example from a Permian tectonite of the Dome de Barrot in the Alpes Maritimes (France) where veins cut through deformed mudcracks (Fig. 3). The Permian rocks of the Alpes Maritimes (France) consist of a sequence of continental redbeds that accumulated in discrete basins during the earliest phases of the breakup of Pangaea (Faure-Maret 1955). During the Miocene Alpine orogeny, these redbeds were coupled to basement deformation under a cover detaching along Triassic evaporates (Goguel 1936). Because of this coupling to basement, strain in the Permian redbeds is believed to be comparable to Alpine strain in the basement massifs including the Argentera and Maures-Esterel (Siddans *et al.* 1984). The veins of Figure 3 propagated during Alpine deformation.

We use veins as a proxy for joints in this case because the mechanics of vein propagation follow the same physical laws as those for joint propagation (Pollard & Segall 1987). We can draw some general conclusions from Figure 3. First, the veins (i.e. filled joints) seem to have propagated in the y–z-plane of this tectonite, thus raising the possibility that the veins are coaxial with finite strain in these Permian redbeds. If the veins are coaxial with flattening of the mudcracks, both deformation processes may have been driven under the same tectonic stress field and may be contemporaneous. Second, the veins are not all perfectly parallel. Third, the veins do not crosscut nor do they abut. We then wonder whether we are

include a $\sigma = 1.7°$ and $\kappa = 3.2$ (Fig. 1a). Anytime a sample of joint orientations displays a positive κ, there is a stronger probability that the sample comes from a single joint set. The natural variability of joint orientation due to subtle rock inhomogeneities and a stress field that is not perfectly homogeneous gives a $\sigma > 1°$ and tends to blunt an otherwise sharply peaked κ (i.e. > 10).

These measurements were converted to a 3D set by arbitrarily assigning a dip of 90° to all joints. This is not unreasonable based on dip measurements from outcrop faces. Twenty-one draws of four data from the randomly sorted set of 80 data gives an α_{95} of between 1.0° and 5.2°, with a median of 2.0° (Fig. 2a). More than 75% of the time a sample of seven from randomly sorted data gives an $\alpha_{95} < \sigma$. Thus, for a single joint set like the ENE joints in the Middlesex Formation, very little information on clustering of orientation is gained by taking more than seven measurements along a scanline. There may, however, be other reasons for collecting more data. Each random draw of 25 data gives an α_{95} less than the bin size used in field sampling.

A sampling program in a rock as homogeneous as the Middlesex black shale might start with a scanline of nearly 100 measurements. Once σ is defined with this larger sample, then sampling at other outcrops may be limited to the sample size required to define an $\alpha_{95} \leq \sigma$. In the case of the relatively homogeneous Middlesex Formation, seven data are enough. For a perfectly systematic set of planar joints (i.e. the wall in Bizanos) very little information is gained by collecting more than four orientation data provided that a Freiberger compass is used.

Characteristics of joint sets generated during folding

The tectonic conditions during joint propagation within the Middlesex Formation on the Appalachian Plateau favours a population displaying a peaked κ. This joint set propagated by hydraulic fracturing in a stress field consistent with Acadian or early Alleghanian deformation to the east (Engelder *et al.* 2001; Lash *et al.* 2004). The black shale was undisturbed by Acadian deformation. There are other tectonic settings where the stress field is not expected to be as homogeneous nor is the host rock as isotropic and homogeneous as the black shale of the Middlesex Formation. Local inhomogeneities in the stress field are expected near faults and folds.

Limb of a large detachment fold

In the Appalachian Valley and Ridge of Pennsylvania, the Brallier Formation is the distal turbidite sequence sitting at about the same stratigraphic position as the Middlesex Formation on the Appalachian Plateau. Near Huntington, Pennsylvania, the Brallier has been folded into the foreland limb of the Broadtop syncline (Ruf *et al.* 1998). Folds of the Valley and Ridge have sharp hinges (e.g. Faill 1973) typical of fault-bend folds (e.g. Suppe 1983). The fine-grained sandstone beds of the Brallier carry a well-developed joint set that parallels the strike of the larger-scale structures. The population of strike joints have a vector mean pole that makes an angle of roughly 85° to pole to bedding in the NW limb of the Broadtop syncline (Ruf *et al.* 1998). This non-orthogonality is interpreted to reflect a stress field that developed below a neutral fibre as the beds were passing through the sharp synclinal hinge going into the hanging-wall ramp at the trailing edge of a horse in lower Palaeozoic carbonate rocks of the Valley and Ridge (Ruf *et al.* 1998).

The stress field in the hinge of chevron folds like those of the Appalachian Valley and Ridge is controlled by bending stresses and, thus, is local rather than being regional, as was the case during propagation of joints in the Middlesex black shale. Depending on exactly when and where the joints propagated with respect to the hinge of the chevron fold, a population of strike joints could have a much larger σ than found in the black shale of the Appalachian Plateau. Strike joints in one bed of the Brallier display $\sigma = 6.1°$ and $\kappa = -0.05$ (Fig. 1b). A negative κ and a large σ are both consistent with jointing in an inhomogeneous stress field. There is no sign that this collection of joints comes from more than one set.

Twenty-one draws of four data collected at random from the Brallier measurements give an α_{95} between 4.0° and 11.2°, with a median of 7.2° (Fig. 2b). For 21 draws of 10 data collected at random, $\alpha_{95} < \sigma$. Although 10 data are enough to define the mean pole for strike joints in the Brallier based on $\sigma = 6.1°$, there are instances in which larger samples are appropriate. For example, we may wish to know if the strike joint set is coaxial with the fold axis. The answer to this question may require an orientation data set large enough to reduce the α_{95} to within $\pm 1°$. Fifty data reduces α_{95} to $\pm 1.4°$, which may be good enough because we see that the mean pole is within 1.4° of the local fold axis as defined by the strike of bedding at Huntington.

Limbs of two basement-cored folds

Basement-cored folds of the Laramide style found in the Rocky Mountains develop in a manner that is consistent with the trishear model for folding (Erslev 1991). The difference between a trishear fold and fault-bend folds of the Appalachian Valley and Ridge is that fold hinges are not as sharp and the fold

field conditions, strike (or dip direction) is commonly read to the nearest degree but it can be read, arguably, to the nearest tenth of a degree with a steady hand under laboratory conditions (i.e. sitting at a desk with no flies and no wind). With a Freiberger compass under field conditions, the dip of a surface is commonly read to the nearest degree but under laboratory conditions dip can be read to the nearest half degree.

To develop a sense for sampling error, the orientation of the inside plaster wall of a 19th century house in Bizanos, France, was measured 50 times. The hinged plate of the Freiberger compass (7×7 cm) was positioned at the same point (±1 cm) on a slightly tilted wall. Strike was read to 0.1° and dip read to 0.5°. A 2D version of these data (i.e. strike data only) is presented as a histogram in both field format with 1° bins and in laboratory format with 0.1° bins (Fig. 1i, j). A $\sigma = 0.2°$ is the statistic that we use to describe the clustering of repeated measurements using a Freiberger compass and a measure of the precision of the Freiberger compass. Because this is such a tight cluster relative to the smallest sample interval (i.e. bin size) used for field measurement, we conclude that the instrument error has negligible impact on field sampling.

Kurtosis, κ, is another instructive statistic (Walpole & Myers 1993). When the compass calibration data is binned in 1° intervals, it possesses a strong positive κ (>23). This, then, would be a characteristic of a systematic joint set propagating in an isotropic, homogeneous medium driven under the influence of an homogeneous stress field. The κ (= −0.57) arising from reading the instrument to 0.1° is negative. A flat orientation distribution is consistent with the inference that strike data cannot be consistently read to the nearest 0.1° on the Freiberger compass, otherwise these data would also possess a positive κ.

There is the question about how much data are enough to define clustering within the population of a single joint set. Again, there is no right or wrong answer to this question. We can start to develop a sense of the degree of clustering using the cone of confidence (McElhinny 1964; Silliphant *et al.* 2002). A cone of confidence indicates the angular distance from the mean pole within which the true pole is found to a certain level of confidence. For example, the statistically averaged dip of the interior wall in Bizanos is 86.01° after 50 measurements, but the true average vector mean dip is somewhere in the range 86.01° ± 0.14° as measured by the 95% cone of confidence (α_{95}). The statistic, $\alpha_{95} = 0.14°$, is a measure of the precision of our sampling instrument based on 50 samples (Fig. 2i). We have no independent measure of the orientation of the wall in Bizanos, so the accuracy of the measurement instrument cannot be assessed.

We can see how a smaller sample impacts on our assessment of instrument precision and then the clustering of a population of poles to joints. For the compass calibration, we selected a small number of data from our randomly sorted collection of 50 measurements. We repeated this random sort 21 times, sampled the same number of data (i.e., four or seven or 10 or 15 or 25 or 35 or 50) after each sort, and calculated a 95% cone of confidence (α_{95}) for each draw. The α_{95} data for each set of 21 similar samples are then sorted for plotting as a box and whisker diagram showing the highest α_{95}, the 75th percentile α_{95}, the 25th percentile α_{95} and the lowest α_{95} (Fig. 2i). With just four random samples 21 times, the α_{95} for our compass calibration varies anywhere from 1.1° to 0.14° with a median of 0.49°. This range of α_{95} from 1.1° to 0.14° is one measure of the degree of clustering of our calibration data. Thus, if a perfectly planar, systematic joint set was encountered in the field, the probability of calculating an $\alpha_{95} \leq 0.49°$ with four measurements using a Freiberger compass is 50%. The probability of calculating $\alpha_{95} \leq 0.49°$ with 10 measurements is $\geq 95\%$. This method of estimating errors is similar to those techniques known in statistics as 'bootstrap techniques' (Efron & Gong 1983; Fisher *et al.* 1987).

The cone of confidence can be compared with 2D strike data for which $\sigma = 0.2°$. When just four samples are taken, most of the clusters of four data will have an α_{95} outside one standard deviation (1 SD) from the mean for the strike data. With 25 samples of our randomly sorted data, more than half of the draws yield an α_{95} within 1 SD of the mean from the 2D data. With 35 samples, each draw yields an α_{95} within the 1 SD. In effect, after 35 samples we have defined the orientation of the wall of the house in Bizanos at the 95% confidence level within the limits of the precision of the instrument.

Clustering of a single joint set independent of tectonic deformation

We wish to define the degree of clustering of poles to a joint set associated with propagation in a rock that is as nearly isotropic and homogeneous as possible. The remote stress field must also be as close to homogeneous as possible and the crack-tip stress fields of pre-existing members of a joint set cannot interfere with the propagation of infilling joints (cf. Olson & Pollard 1989). Natural hydraulic fractures infill without interference from the crack-tip stress field of neighbours (Fischer *et al.* 1995). For this purpose we look to a joint set that cuts black shale of the Devonian Middlesex Formation in the Appalachian Basin (Sheldon 1912). Within this black shale an ENE joint set is the most prominent and it propagated independently of Alleghanian structures (Engelder *et al.* 2001). These are hydraulic fractures with pressures generated during initial maturation of hydrocarbons within the black

changing orientation in time. Finally, we use our statistical analysis to test whether or not a joint set correlates with the orientation of other structures.

Analysis of directional data

There are many ways to present joint orientation data. However, there are some instances when three-dimensional (3D) sampling is not possible (e.g. an outcrop that is a pavement surface). Rose diagrams for 2D data and stereonets for 3D data are two of the most commonly employed plots (e.g. Davis 1986). A qualitative measure of the clustering of orientation data is readily apparent on both plots, although neither allows for testing of statistical hypotheses and neither gives a sense of spatial variation in joint orientation because all data are plotted as if taken from one point. To illustrate spatial variation, ball and stick diagrams are presented on well logs (Narr 1991). Azimuth v. traverse distance plots serve the same purpose for outcrop data (Wise & McCrory 1982). The advantage of the latter, in particular, is that it is very helpful for identification of a single joint set that changes orientation by over several tens to hundreds of metres in terrain where outcrop is limited. Such dramatic swings in orientation are, indeed, a reality for joint sets that have propagated near fault contacts (e.g. Rawnsley *et al.* 1992).

For statistical testing of directional data, the probability model that is most useful is the von Mises distribution, an equivalent to the normal distribution (Davis 1986). Like the normal distribution, the von Mises distribution is characterized by two parameters, the mean direction and a concentration parameter equivalent to the standard deviation. To get a sense of the degree of clustering in 2D directional data, each datum (i.e. the strike of a joint) is assumed to be unit vector at an angle, θ, relative to the x-axis:

$$x_i = \cos\theta_i \text{ and } y_i = \sin\theta_i. \quad (1)$$

The resultant vector from a data set is

$$R = \sqrt{(\Sigma_{i=1}^{n}\cos\theta_i)^2 + (\Sigma_{i=1}^{n}\sin\theta_i)^2} \quad (2)$$

where n is the number of strike measurements. The mean resultant vector, $\bar{R}$, is calculated according to

$$\bar{R} = \sqrt{\bar{C}^2 + \bar{S}^2} \text{ where } \bar{C} = \frac{1}{n}\sum_{i=1}^{n}\cos\theta_i$$

$$\text{and } \bar{S} = \frac{1}{n}\sum_{i=1}^{n}\sin\theta_i. \quad (3)$$

Dispersion of a joint set measured on a pavement surface is measured by the complement of $\bar{R}$, the circular variance,

$$s_o^2 = 1 - \bar{R} \quad (4)$$

This leads directly to a confidence angle around the mean strike of the sample (Davis 1986). For data that are normally distributed about a mean, with sample ranges having a small angular variation, the square root of the circular variance is similar to standard deviation in a normal distribution (Mardia 1972).

The clustering of 3D data is characterized by a cone of confidence, a statistic that was developed to describe dispersion on a sphere (Fisher 1953). The cone of confidence measures the probability, P, that the actual mean pole of a joint set sits outside the cone measured from the calculated mean pole, based on the sample size of N joints. α_{95}, the cone outside of which there is only a 5% probability that the true mean pole sits, is calculated from

$$\cos\alpha = 1 - \frac{(N-R)}{R}\left\{\left(\frac{1}{P}\right)^{1/1-N} - 1\right\} \quad (5)$$

where $N = n$. R, as in the 2D case, is the sum of the vectorially added individual unit vectors, such that $R \leq N$.

While the clustering of joint-orientation data is best assessed using the cone of confidence (equation 5), we also reduce scanline data to 2D sets as if we measured the strike of joints on a pavement surface where the third dimension was inaccessible. Assuming a von Mises distribution with an angular variation that is equivalent to standard deviation, σ, we calculate σ and kurtosis, κ, of these 2D data using the standard statistical package on Microsoft Excel. Kurtosis is a measure of the deviation of a data set from an ideal normal distribution. A positive κ means that the data distribution is more peaked than a normal distribution, whereas a negative κ means the data are flatter than a normal distribution (Walpole & Myers 1993). This measure of the distribution of joint orientation data is worth exploring despite being somewhat ad hoc because systematic joint sets, planar and parallel, will have a large positive κ. A negative κ will be the signal that the joints are not systematic or that more than one joint set is being measured.

Calibration of the Freiberger compass

Because sampling techniques are not perfectly reproducible, sampling will affect the distribution of joint orientation data even if the joint population is perfectly systematic. Orientation data collected for this chapter were taken along scanlines using a Freiberger compass. The flat plate on the back of the Freiberger compass is perfectly suited for measuring planar surfaces with both dip and strike data collected during a single contact between compass and outcrop. Under